Deformation rates and localization of an active fault system in relation with rheological and frictional slip properties: the Corinth Rift case

S. El Arem[1,*], H. Lyon-Caen[1], P. Bernard[2], J-D. Garaud[3], F. Rolandone[4], P. Briole[1]

(1) Laboratoire de Géologie, Ecole Normale Supérieure CNRS, Paris, France. (2) Institut de Physique du Globe de Paris, France.
(3) Onera - The French Aerospace Lab, F-92322 Châtillon, France. (4) ISTeP, UPMC, CNRS, Paris, France
(*) Contacts: elarem@geologie.ens.fr

I. CONTEXT AND AIM OF THE STUDY

The Corinth Rift in Greece is one of the most active extensional regions in the Mediterranean area (**Fig. 1**). The Corinth Rift Laboratory project (CRL, http://crlab.eu) is based on the cooperation of various european institutions that merge their efforts to study fault mechanics and related hazards in this natural laboratory where numerous continuous observations are made. The present rift is asymmetric and deformation is very localized. Numerous GPS campaigns since 1991 indicate a stable opening rate of about 1.5 cm/yr over a width of 10- 12 km in the western part of the rift (**Fig. 2**). Continuous GPS stations installed 10 years ago start to reveal reliable vertical displacement (**Fig.3**). The seismic activity is localized in the upper 12 Km of the crust. Although the 3D geometry of active faults might be quite complex (**Fig. 4**), we present here a simple 2D mechanical model including one normal fault embedded in an elasto-visco-plastic medium, aimed at exploring crustal rheology and fault parameters able to explain both horizontal extension rates and vertical deformation.
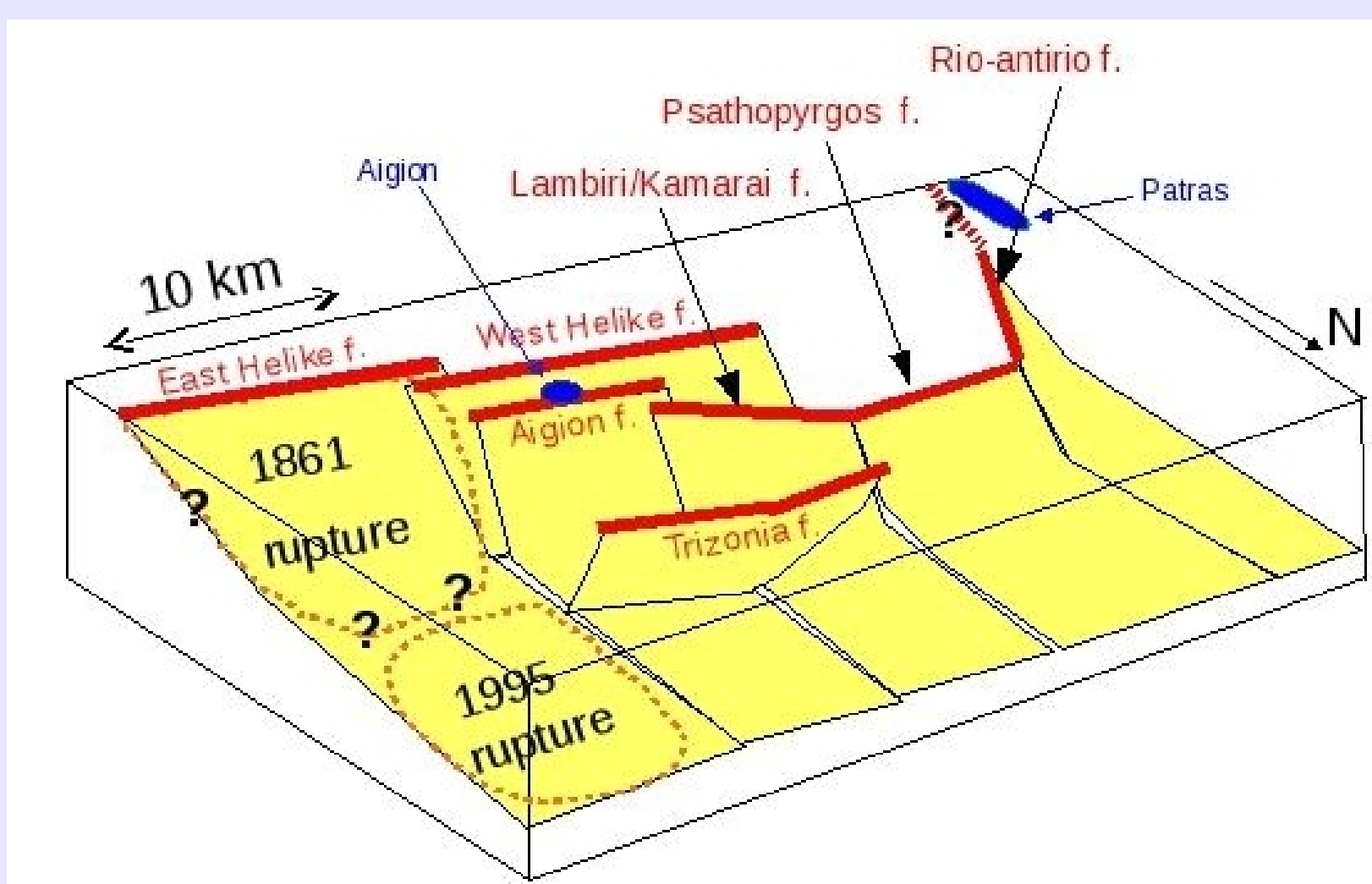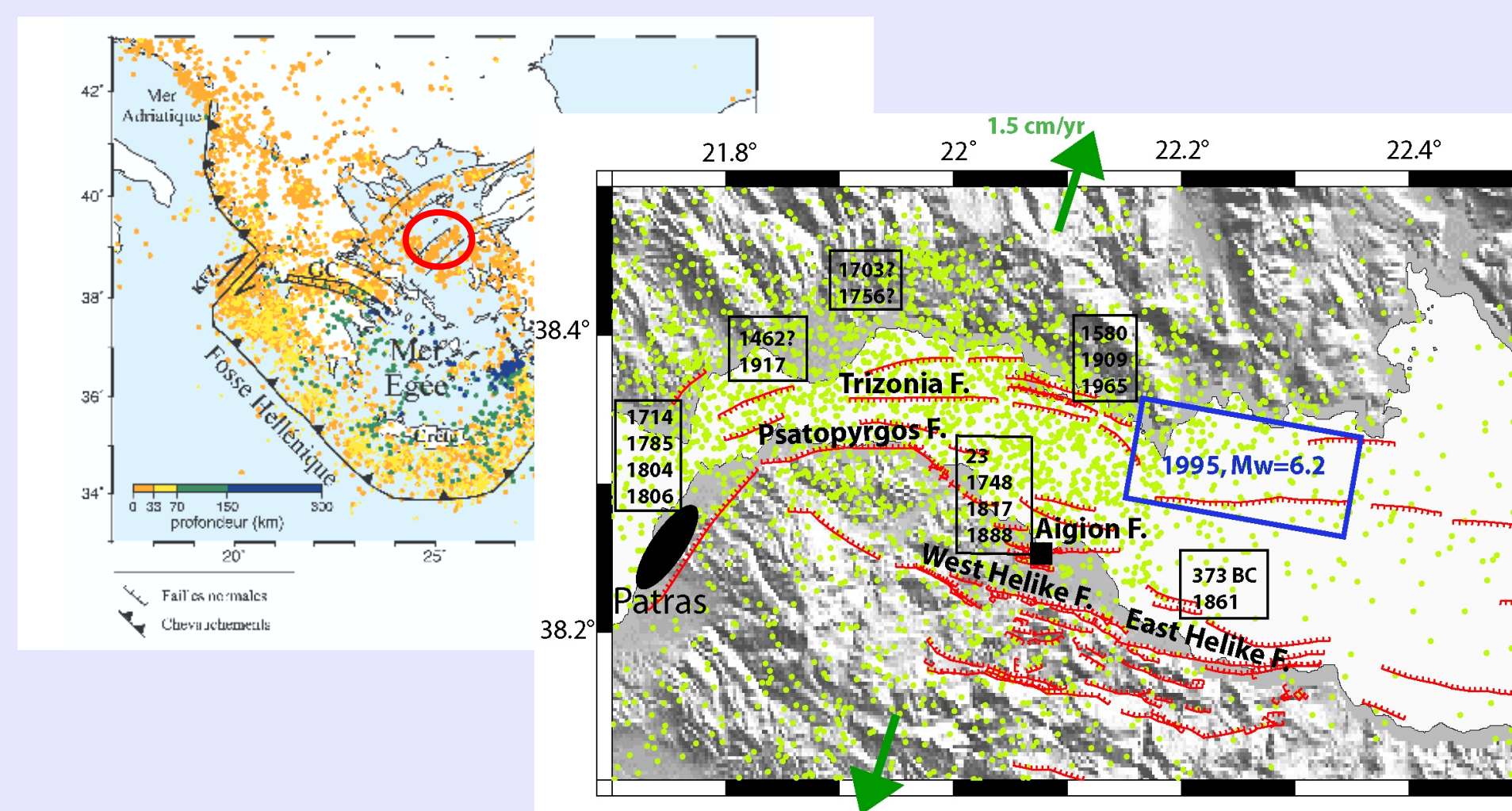

Figure1. seismotectonic context of the western rift of Corinth, with faults and seismicity. Green dots: seismicity 1964-2008, from National Observatory of Athens (M>3,depth 0-20 km). Blue rectangle: Aigion 1995 earthquake area. Red: major active faults.
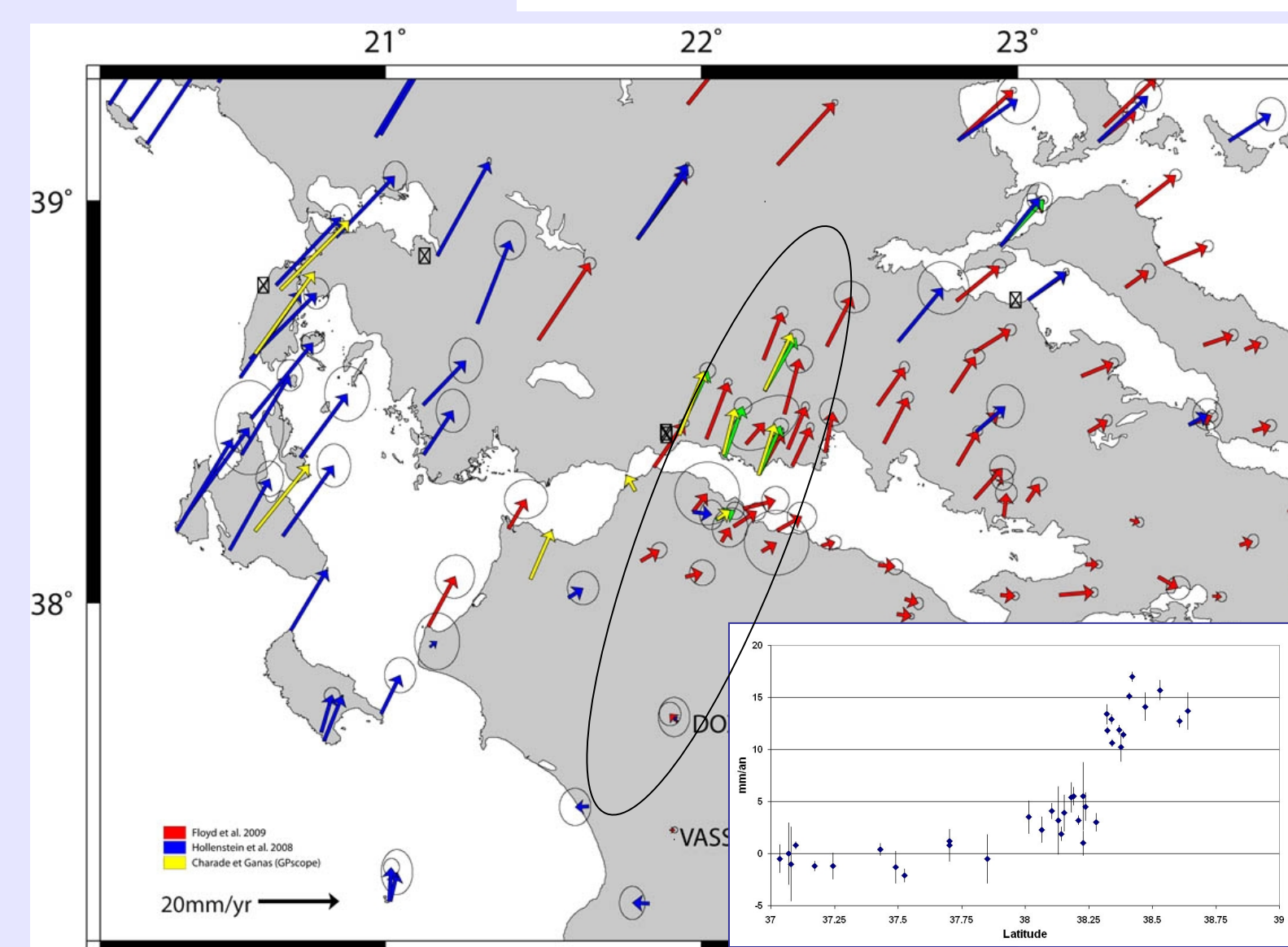

Figure 3. Vertical displacement at TRIZONIA island continuous permanent station, close to the northern coast of Corinth rift.

Figure 4. 3D sketch of major active faults in the study area

Figure 2. GPS horizontal velocity field with Peloponissos fixed obtained from compilation of various observations since 1991 (from E. Perouse).
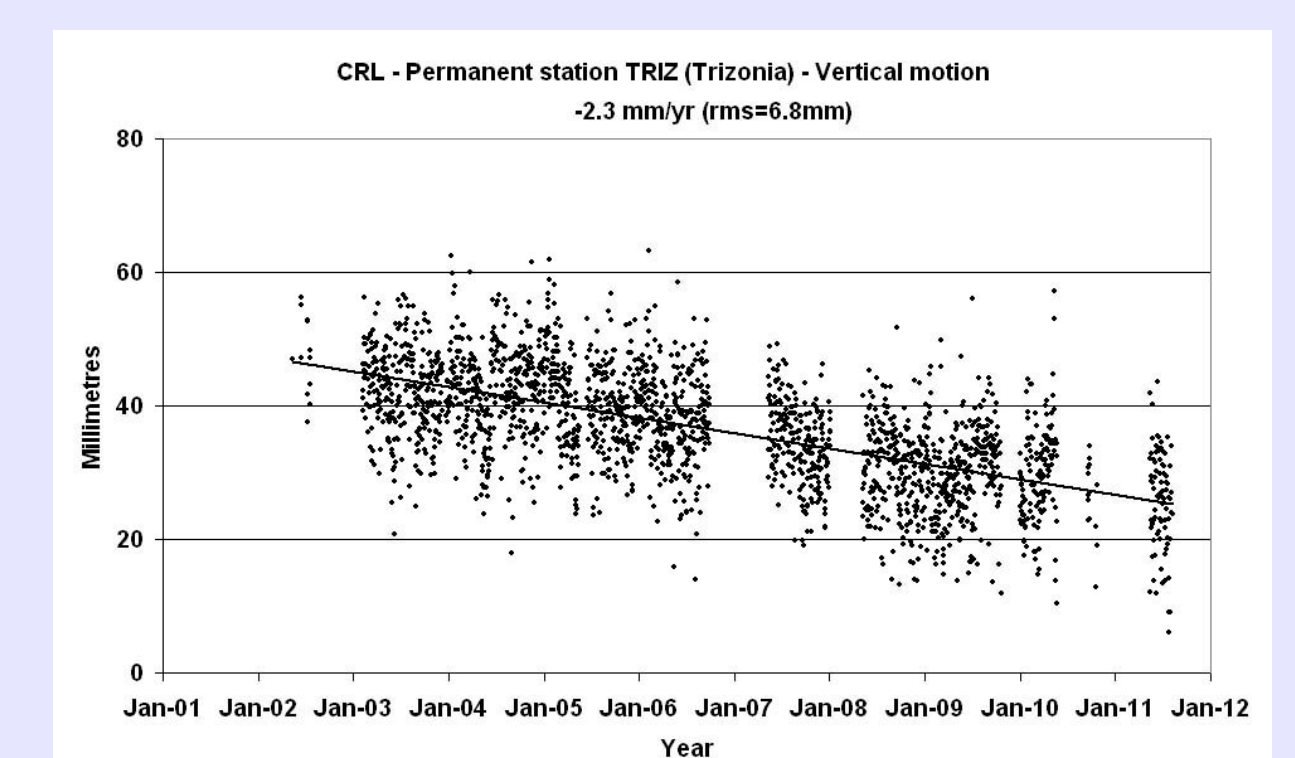
Our purposes with this simple 2D model are:

1. To constrain the upper crust rheology by modelling the available deformation data (horizontal and vertical GPS velocities).
2. To explore the effects of the crustal rheology and fault parameters on the stress and strain distribution at depth.

II. Model

1. Rheology: A Maxwell-extended model rheology is considered in this work (**Fig. 5**). The hydrostatic stress dependence in crustal rocks is accounted by considering the Drucker-Prager plasticity criterion. Thus, the yield surface is: $F = q - P * tan(\beta) - d$ with β the friction angle and **d** the cohesion. $P = -1/3 * trace(\sigma)$ is the hysrostatic pressure and $q = \sqrt{(1/2 * S:S)}$ the Von Mises equivalent stress. The potential flow is described by: $G = q - P * tan(\psi)$ with ψ the dilatation angle. In this work, we consider an associated flow rule: $\psi = \beta$ (**Fig. 6**).

2. Finite Element model: Our 2D model represents a NNE-SSW cross section across the rift. It extends down to 40 km and is 108 km long (**Fig. 7a**). We consider a linear vertical temperature gradient of **16°C/Km** (**Fig. 7b**).

Finite element mesh: We consider linear elements with a resolution of **300 m** in the fault area that decreases to **2~3 km** along the boundaries.
Loading: The model is submitted to the effects of gravity and a horizontal extention of **1.3cm/yr.**
Mechanical modelling: plane strain approximation in the finite strain framework is considered, and contact conditions with Coulomb constant friction on the fault lips.
Creep: viscous power-law rheology: $\dot{\epsilon}^v = A\, q^n\, exp(-Q/RT)$, $n = 3.1$, $A = 2.10^{-21}\, Pa^{-n}\, s^{-1}$, $R = 8.314$, $Q = 152\, KJ\, mol^{-1}$
With these parameters, the **brittle-ductile** transition occurs at approximately 8Km depth (**Fig. 7c**).
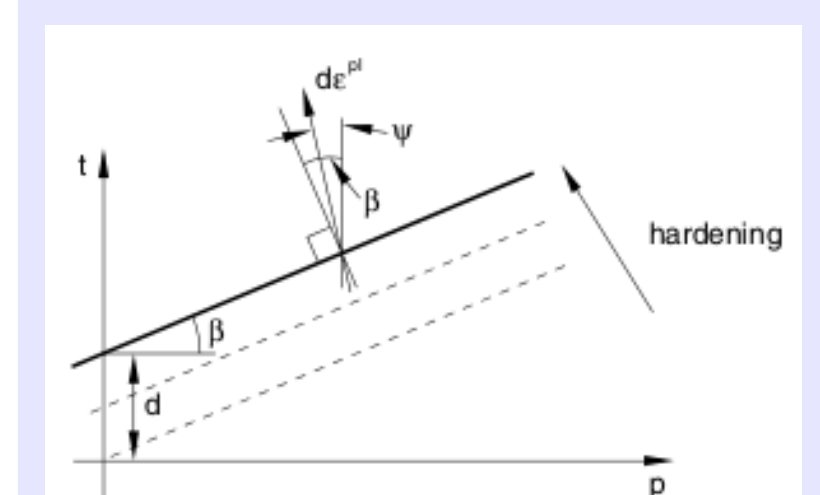

Figure 5. Rheological model

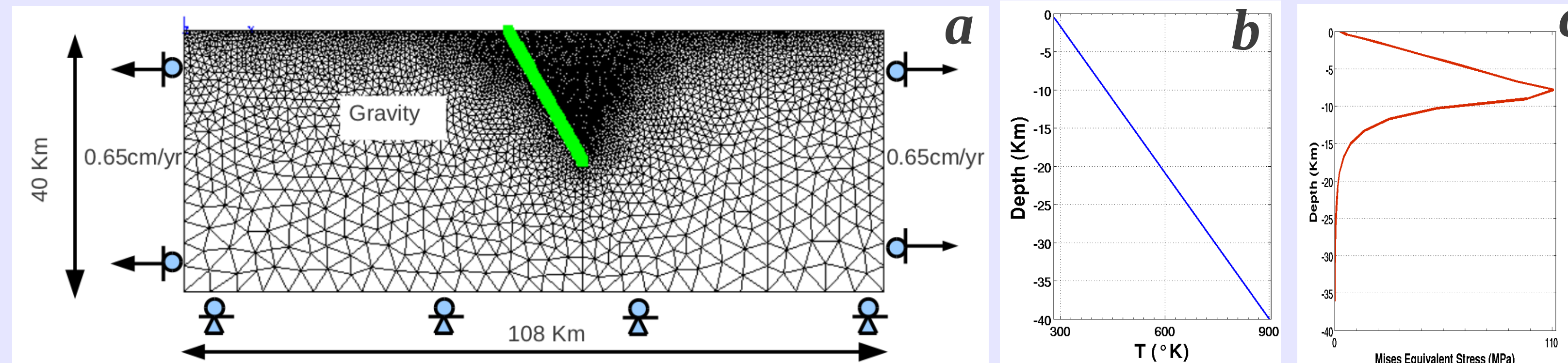*Figure 6. Yield surface and flow direction*

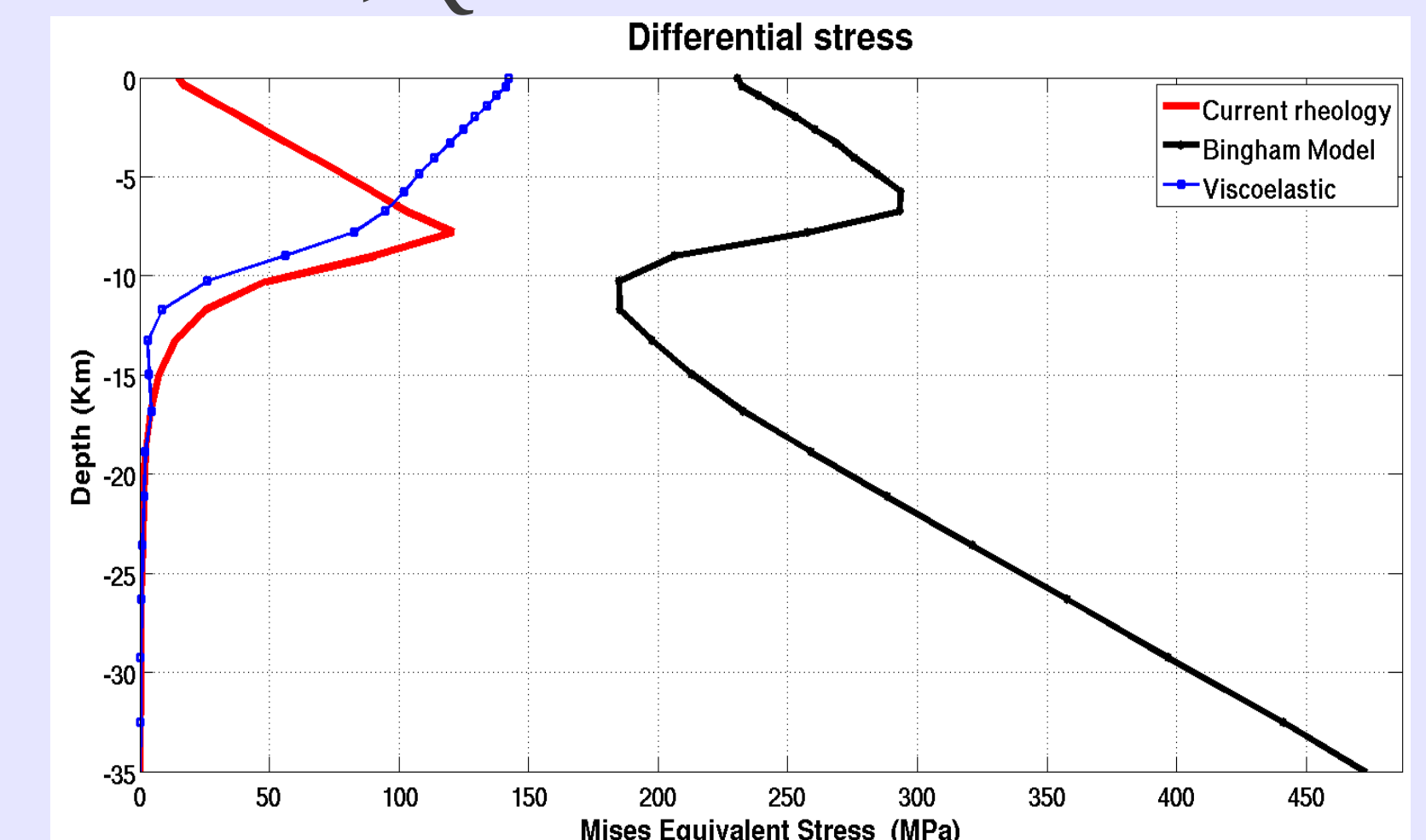*Figure 7. (a) FE Model, loading and BC (b) linear vertical T gradient and (c) Vertical differential stress q*

Figure 8. The vertical differential stress for the current rheology, the Bingham's generalized model (with de dashpot in parallel with the plasticity friction element), and a viscoelastic rheology (no plasticity).

III. MAIN RESULTS

1. Differential stress: Activation energy influence
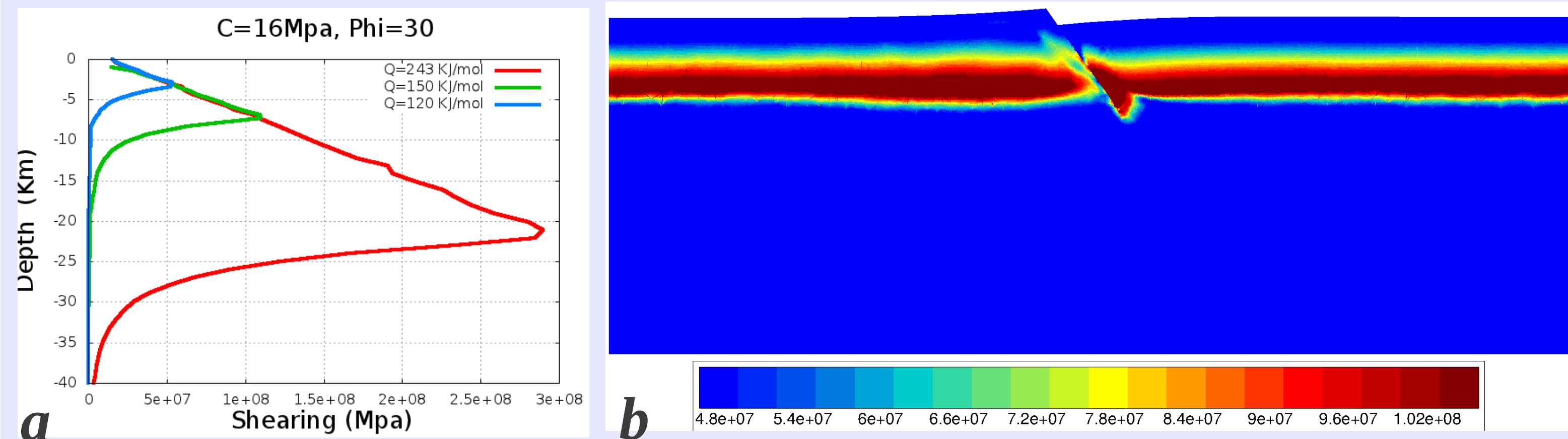

Figure 8. (a) Differential stress (DS) as a function of the activation energy Q. The DS distribution reflects the brittle and viscous rheologies prevailing in the upper and lower crust, respectively. The brittle-ductile Transition Depth (TD) decreases with decreasing Q (b) Distribution of DS for Q=150KJ/mol marking the transition from brittle to ductile behavior at a depth of about 8 Km.
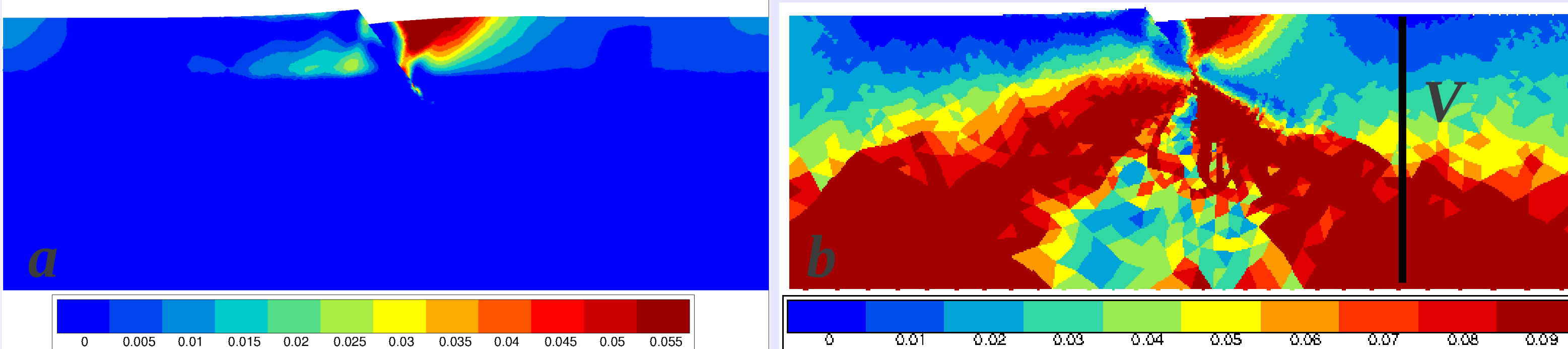
2. Plastic deformation localization

Figure 9. Cumulated plastic deformation after 200Ky of extension showing localization close to the fault zone preceeding the appearance of new faults. Qualitatively, frictional-plastic strain accumulates in a triangular wedge of the footwall block and is conspicuously very low within the hangingwall. (b) Total equivalent strain showing localization of viscous strain in the lower zone. Less deformation occurs in the zone beneath the fault since this zone remains under compression for more than 200 Ky of extension at 1.3cm/yr. Q=150KJ/mol, fault depth =15 Km
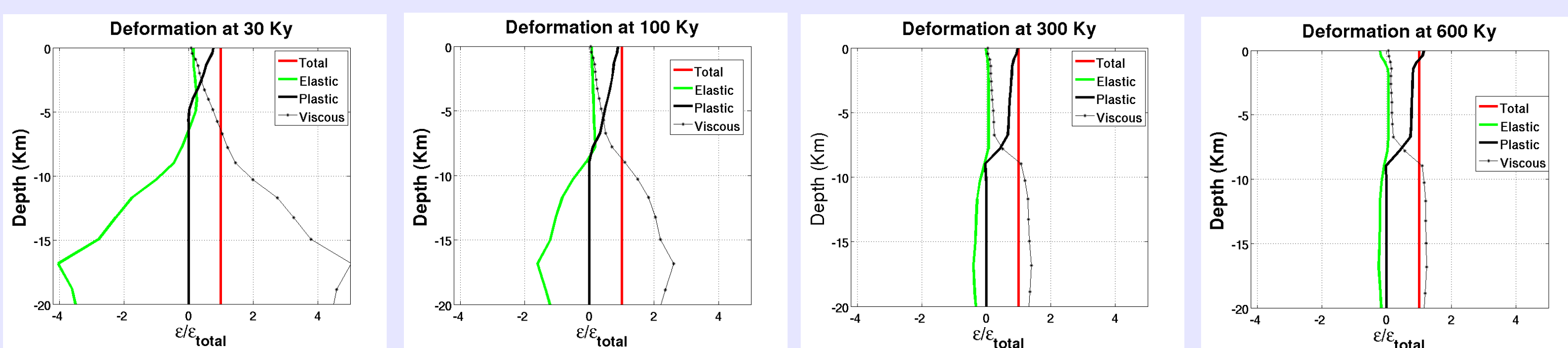
3. Vertical strain distribution

Figure 10. Elastic, plastic and viscous vertical strains evolution with extension time from 30 to 600Ky at 40Km from the fault (vertical line V Fig. 9b). Frictional-plastic deformation accumulates exclusively in the upper crust at depths shallower than the TD (8 Km). Viscous deformation is the dominant contribution to deformation at high temperature and pressure characterizing the lower crust. Q=150KJ/mol, fault depth =10Km.

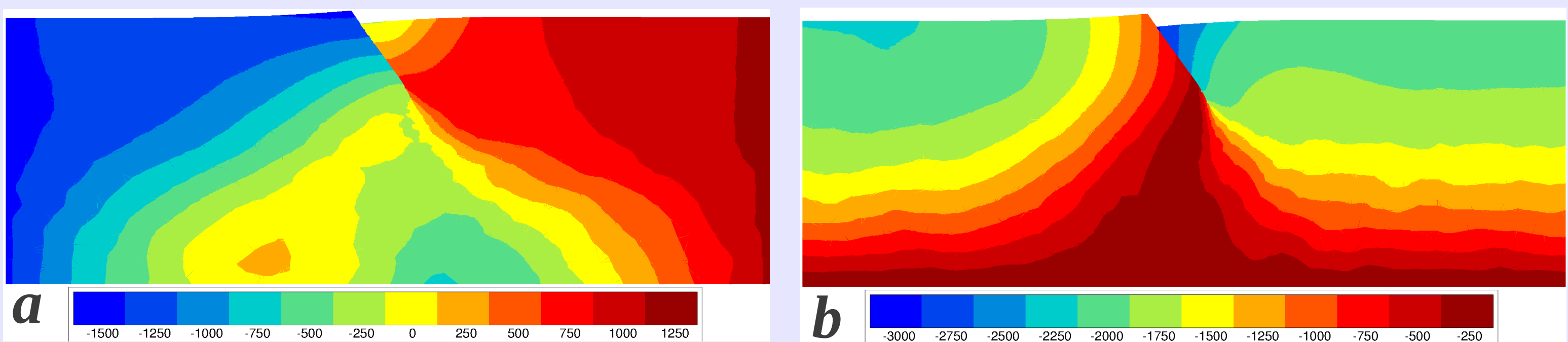## 4. Surface Deformation

Figure 11. Horizontal (a) and vertical (b) displacements distributions showing the discontinuities due to the mouvements of the fault blocks and the slip gradient on the fault.
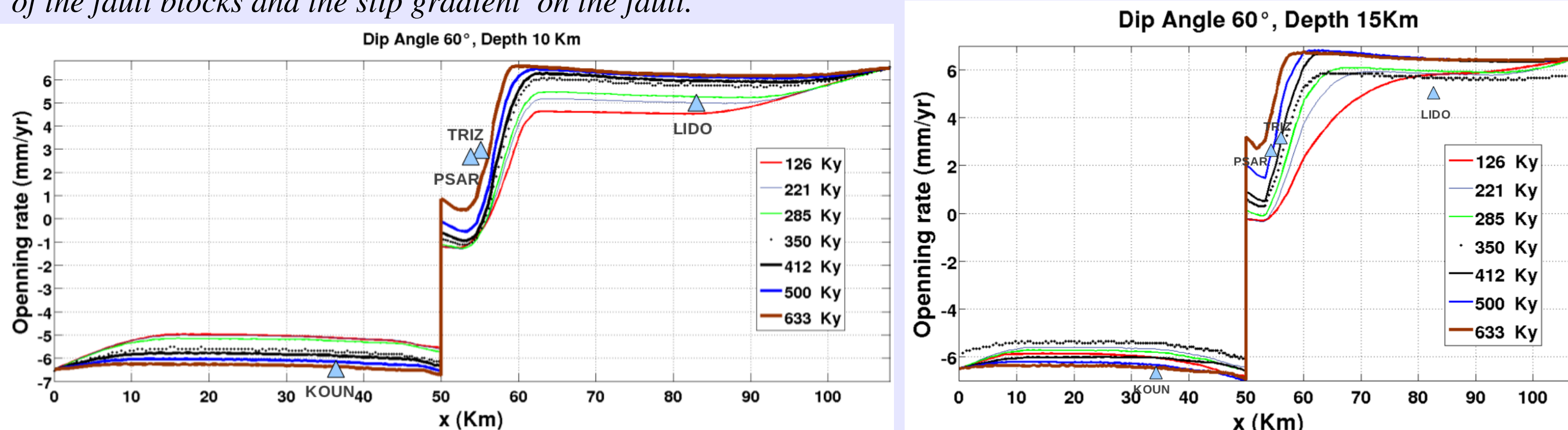

Figure 12. Horizontal GPS velocities vs. computed openning rates for 10 and 15 Km fault depth. For fault depths greater than the Transition Depth (TD), and after 200 to 300 Ky of extension, the major part of surface deformation is localized around the fault zone.

Bibliography

- P. Bernard et al. "Seismicity, Deformation and seismic hazard in the western rift of Corinth : New insights from the Corinth Rift Laboratory (CRL)", Tectonophysics 426 (2006) 7 – 30.
- Cianetti et al.," Modelling deformation rates in the western gulf of corinth: rheological constraints" Geophys. J. Int. (2008) 174, 749-757
- Dempsey et al.," the role of frictional plasticity in the evolution of normal fault systems" J. Structural Geology, 2012
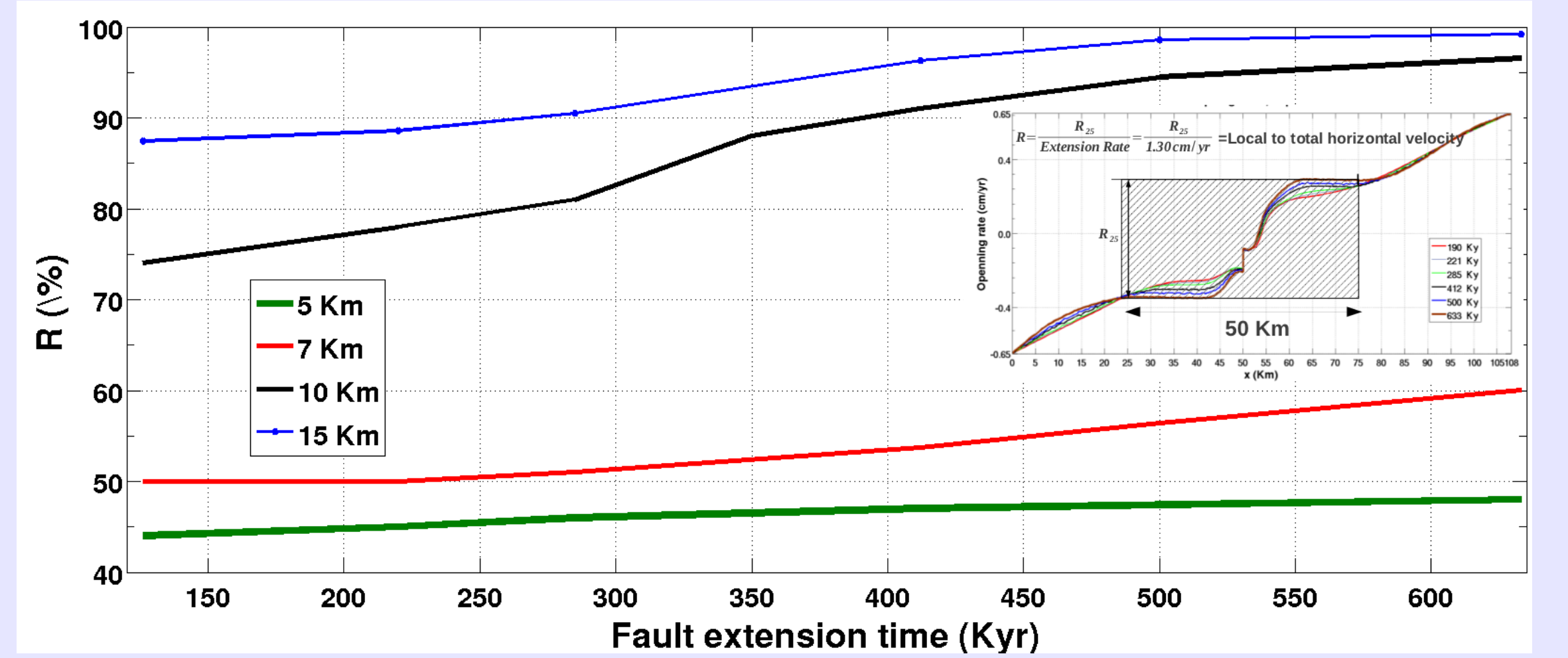
5. Localization of horizontal deformation

Figure 13. Evolution of the local to total opening rate: R=R25/(total extension rate). R25 is the local extension rate measured within 25 Km from the fault. For a fault with depth less than the TD (5 and 7 Km), R never exceeds 60% even after 600 Ky of extension. For deeper faults, R reaches high levels (> 75%) at a relatively early stage of the process.
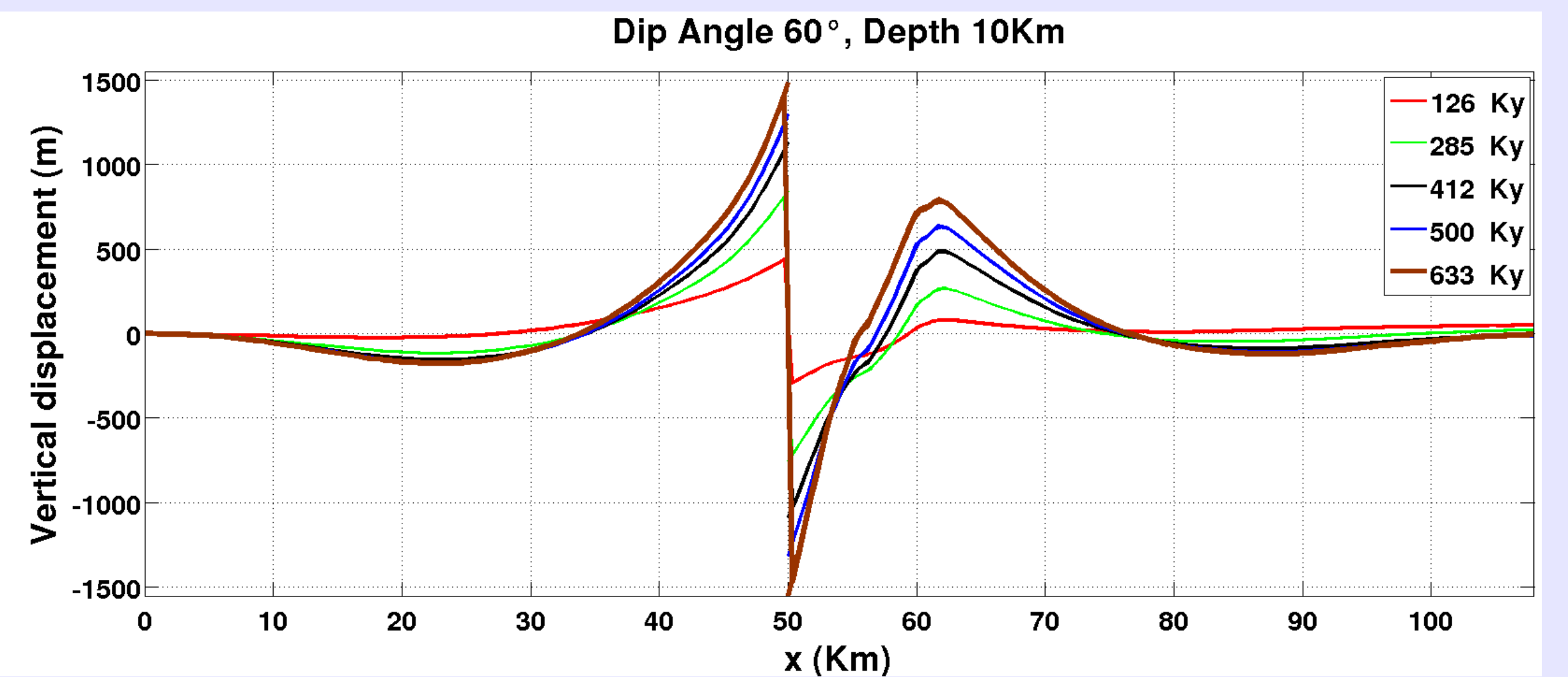
6. Surface vertical Deformation

Figure 14. Vertical displacement showing an uplift in the south and subsidence in the north of the CR.
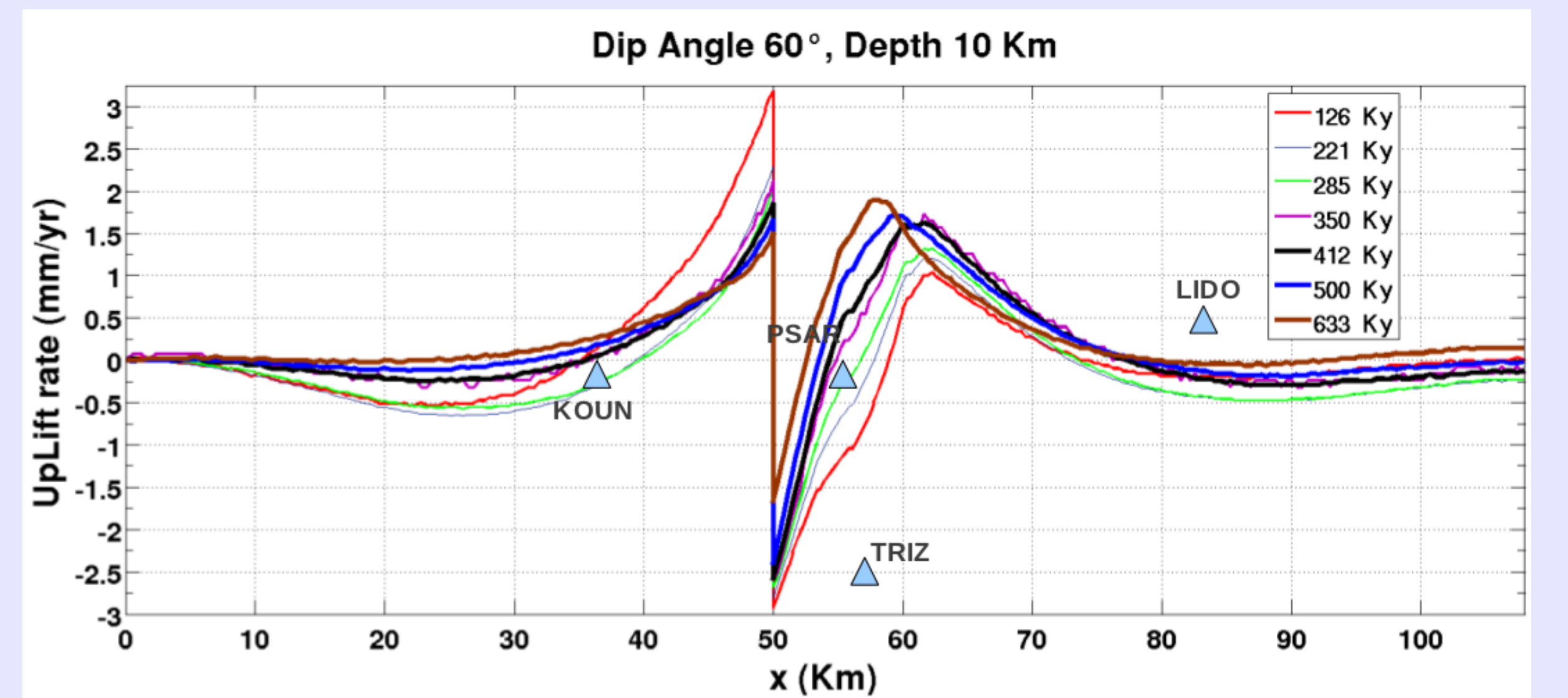

Figure 15. Vertical Velocities (VV). It appears that VV at TRIZ can not be reproduced by this simple model because it is likely to be affected by the presence of secondary faults.

IV. CONCLUSIONS

A 2D plane strain model is considered to investigate the extension and subsequent deformation within the brittle crust. In addition to dip-slip on the fault contact surface, extension mechanism leads to an accumulation of plastic deformation within the upper crust. Below the brittle-ductile transition depth, both plastic strain and fault slipping decrease rapidly. The viscous deformation prevails in the lower crust.

In order to explain both horizontal and vertical surface deformation velocities, and depth range of seismic activity (<12Km), the following conditions should be met:
A/ a brittle to ductile transition depth (TD) shallower than 12 Km
B/ A fault depth greater than the TD

Moreover, the evolution towards a symmetric profile of the computed vertical velocity (as shown in Fig. 15) is not consistent with the field observations. This finding implies that the normal fault system active in the western corinth rift is quite young (<200Ky).